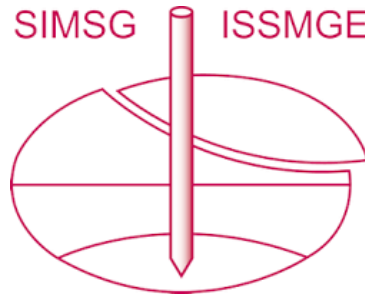


INTERNATIONAL SOCIETY FOR SOIL MECHANICS AND GEOTECHNICAL ENGINEERING



This paper was downloaded from the Online Library of the International Society for Soil Mechanics and Geotechnical Engineering (ISSMGE). The library is available here:

<https://www.issmge.org/publications/online-library>

This is an open-access database that archives thousands of papers published under the Auspices of the ISSMGE and maintained by the Innovation and Development Committee of ISSMGE.

The paper was published in the proceedings of the 10th European Conference on Numerical Methods in Geotechnical Engineering and was edited by Lidija Zdravkovic, Stavroula Kontoe, Aikaterini Tsiampousi and David Taborda. The conference was held from June 26th to June 28th 2023 at the Imperial College London, United Kingdom.

To see the complete list of papers in the proceedings visit the link below:

<https://issmge.org/files/NUMGE2023-Preface.pdf>

Validation of a new constitutive model with reversal surfaces for the analysis of liquefaction-induced phenomena

T.G. Limnaiou^{1,2} and A.G. Papadimitriou²

¹*GR8 GEO, Engineering consultants, Athens, Greece*

²*National Technical University of Athens, Athens, Greece*

ABSTRACT: This paper presents the validation of a new constitutive model with reversal surfaces in accurately predicting the soil response in boundary value problems (BVPs) related to liquefaction. The new model, named *LiPa* model, has been implemented in finite difference codes *FLAC* and *FLAC3D*, via their User-Defined-Model mode, for numerical analyses in the 2D and 3D space respectively. The validation of the new model is presented for two BVPs of slightly inclined liquefiable soil profiles susceptible to lateral spreading, including: a) the seismic response of a uniform liquefiable sand layer and b) the simulation of a pile group response in a three-layered liquefiable soil profile. The validation is based on comparisons with measurements from centrifuge experiments, where Nevada sand is used as the basic sand material. In both studied cases a unique set of model constants is adopted, that is derived after a thorough calibration against monotonic, dynamic and cyclic element tests on Nevada sand. It is shown that the new model can predict qualitatively, but also quantitatively, all aspects of the response, namely ground accelerations, excess pore pressures and ground (and pile) displacements with a single set of model constants and by following the same numerical methodology, despite the different case-specific conditions.

Keywords: Liquefaction, Constitutive modeling, Numerical analyses, Lateral spreading, Piles

1 INTRODUCTION

Advanced numerical analyses of boundary value problems (BVPs) in geotechnical engineering rely, among others, on the use of an appropriate constitutive model for the geomaterial at hand, which is properly calibrated and has been verified against experimental data for various loading conditions. For granular soils (e.g., sands) users commonly employ different constitutive models and/or different calibrations of the same model, depending on the examined loading conditions (e.g., monotonic vs cyclic). Moreover, quite important for the numerical accuracy is to ensure that the employed model is validated not only against element tests, but also against data from multiple BVPs.

Recently (Limnaiou and Papadimitriou, 2023a, 2023b) proposed a new general-purpose bounding surface plasticity model (named *LiPa* from the surnames of the authors) that targets to capture accurately both the monotonic (up to the critical state) and the cyclic response of granular soils (for any shear strain level) with a single set of soil-specific constants for any relative density, stress level and loading conditions. It is a SANISAND-type model with reversal surfaces, that inherits elements from the NTUA-SAND model (Andriopoulos et al. 2010). It includes a macroscopic constitutive scheme for post-liquefaction strain accumulation, as well as an algorithm for avoiding stress-strain overshooting. The foregoing papers also present the calibration process and a thorough validation against element

test data on different sands (Toyoura, Ottawa-F65, Nevada and Monterey) and gravels (Pea gravels), as well as against empirical relations quantifying different aspects of element response (e.g., shear modulus degradation and hysteretic damping increase with strain level: Darendeli 2001; strain accumulation in drained cyclic loading: Bouckovalas et al. 1984). Indicative pertinent comparisons can also be found in the accompanying paper of Limnaiou and Papadimitriou (2023b) in this conference that focuses on the model's formulation.

For its complete validation to be achieved, the *LiPa* model was implemented in numerical codes *FLAC* and *FLAC3D*, via their User-Defined-Model mode, thus enabling numerical analyses in the 2D and 3D space respectively. In Limnaiou and Papadimitriou (2022), multiple BVPs in the 2D space involving seismic liquefaction were presented, with focus on the seismic response of: a) the free-field (horizontal and inclined liquefiable sand layers) and b) single footings (on single-layered or two-layered liquefiable soil profiles). Herein, the numerical validation focuses on the seismic response of mildly inclined liquefiable layers undergoing lateral spreading through comparisons for: a) a uniform layer in 2D space and b) a pile group response in three-layered soil profile in 3D space.

2 VALIDATION AT ELEMENT LEVEL

In this paper, the model validation employs mainly Nevada sand and covers not only element tests, but also

BVPs on the basis of dynamic centrifuge test data. For this purpose, a unique set of values for the 14 model constants is selected and presented in Table 1.

Table 1. Values of model constants for Nevada sand

Constitutive part	Parameter	Values
		Nevada sand
Elasticity	G_o	500
	ν	0.15
	e_{ref}	0.875
	λ	0.079
	ξ	0.19
CSL	M_c^c	1.25
	c	0.74
	n^b	1.1
Plastic modulus	h_o	235
	c_h	4
	n^d	1.2
Dilatancy	A_o	2.6
Fabric	N_o	4400
Post-liquefaction	L_o	750

Figures 1 and 2 present comparisons of model simulations to element test data for Nevada sand, focusing on the undrained cyclic response and the liquefaction resistance, which are of major importance for the examined BVPs. Specifically, Figure 1 shows the model performance for one undrained cyclic simple shear test performed on Nevada sand by Arulmoli et al. (1992) to a sample with relative density $D_r = 60\%$ consolidated at an initial axial effective stress $\sigma_{a,o} = 160$ kPa. The single amplitude of the cyclically applied shear stress τ_{cyc} equals to 26.2 kPa. The comparison is made in the spaces of shear stress τ vs effective axial stress σ_a (Figures 1a, c) and τ vs shear strain γ_{SS} (Figures 1b, d). Observe that the model captures quite well the cyclic response of Nevada sand, including the post-liquefaction shear strain accumulation. In addition, Figure 1e plots the more intense post-liquefaction shear strain accumulation when the parameter $L_o = 75000$, instead of 750 which is the calibrated value (Table 1). Note here that if $L_o = 0$ was used, the amplitude of cyclic strain would essentially “stabilise” at the onset of liquefaction and no further accumulation would be predicted. The exact value of L_o does not affect the stress path, thus the pertinent comparison plot is omitted. This effect of L_o will be discussed, at system level, in the sequel.

As the focus here is on the simulation of BVPs including liquefaction-related phenomena, it is crucial that the model validation compares the liquefaction resistance curves of the data and simulations, i.e., the curves that relate the applied $CSR = \tau_{cyc}/\sigma_{a,o}$ to the number of loading cycles N_l required for liquefaction. Hence, Figure 2 compares the liquefaction resistance curves derived from the available element tests and the respective model simulations. The available data for the examined relative densities of $D_r = 40\%$ and 60% refer

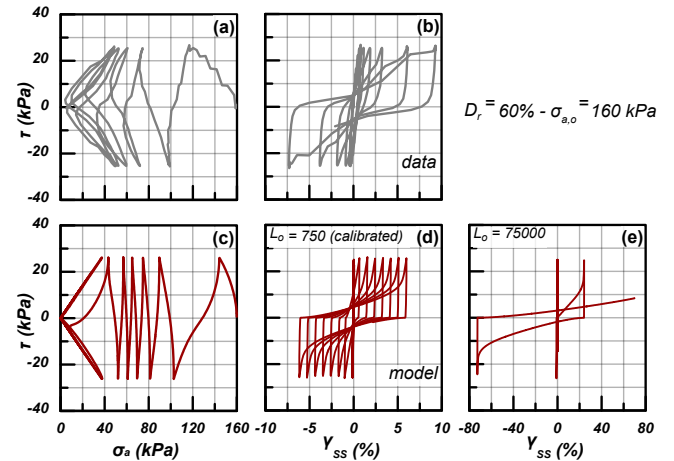


Figure 1. Experimental data versus model simulations of an undrained cyclic simple shear test on Nevada sand

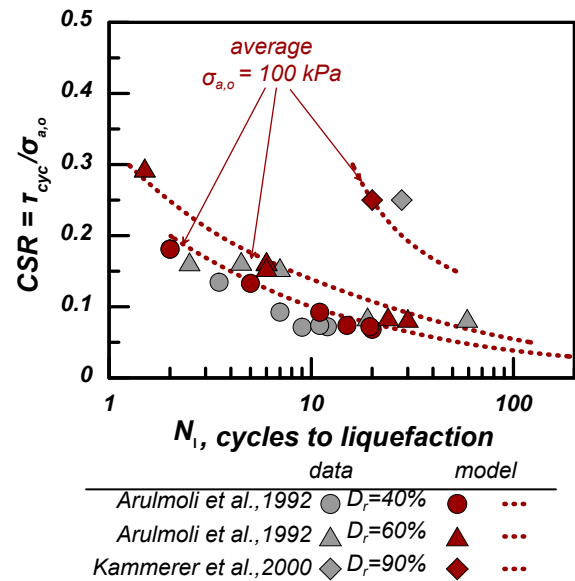


Figure 2. Experimental data versus model simulations of liquefaction resistance curves for undrained cyclic simple shear tests on Nevada sand

to the experimental work of Arulmoli et al. (1992), while the data for $D_r = 90\%$ refer to the experimental work of Kammerer et al. (2000) on the same sand. Specifically, the series of symbols refer to the specific conditions of each test, which were performed for initial axial effective stress values $\sigma_{a,o}$ ranging from 40 kPa to 160 kPa. To clarify the effect of D_r simulated by the model, the figure also includes dashed lines that correspond to a specific value of $\sigma_{a,o}$ ($= 100$ kPa). Observe that the points referring to the simulations generally plot within the range of the corresponding experimental data for different D_r values and, as such, the model simulates satisfactorily the increase of liquefaction resistance with D_r .

3 VALIDATION AT SYSTEM LEVEL

The implementation of the new model in *FLAC* (Itasca, 2011) and *FLAC3D* (Itasca, 2012) allowed its use in the

simulation of BVPs involving the response of liquefiable sand at a system level under dynamic loading. Details about the implementation procedure are presented in Limnaiou and Papadimitriou (2022). For the validation, dynamic centrifuge tests performed on Nevada sand, were employed herein. As such, the new model was used by adopting the calibration of its constants listed in Table 1. By keeping the same values of model constants in both dynamic centrifuge test simulations, this section demonstrates the model's capability to simulate satisfactorily the response of the same granular soil regardless of the BVP in question. For the same reason, the numerical methodology setup was also retained the same in terms of boundary conditions, permeability coefficient for Nevada sand, numerical damping (on top of what the *LiPa* model predicts) and pore fluid bulk modulus in the fully coupled nonlinear dynamic analyses. The numerical methodology is thoroughly described in Limnaiou and Papadimitriou (2022).

3.1 Seismic response of a mildly inclined liquefiable soil layer

The ability of the model to simulate the seismic response of a mildly inclined liquefiable soil layer undergoing lateral spreading is verified here against the experimental data of centrifuge Model test No. 2 of the VELACS project (Taboada and Dobry, 1994). In prototype scale, a 10 m deep uniform Nevada sand layer of approximately $D_r \approx 40\% - 45\%$ relative density is examined. The centrifuge model was built into a laminar box, where the water table was set 1 m above the ground surface and the box was tilted by 2° towards the clockwise direction, thus inducing a uniform mild inclination of the ground surface (see Figure 3a). The input motion was applied at the base of the box and consisted of approximately 20 cycles with a duration of almost 13.5 s, with a peak horizontal acceleration of almost 0.23 g and a predominant frequency of 2 Hz (Figure 3b). The response of the mildly inclined liquefiable ground was monitored along the axis of symmetry of the box, as well as closer to the boundaries, with the installation of accelerometers (AH3), pore pressure transducers (P5, P6, P7) and LVDTs (3, 4, 5, 6) measuring displacements. The model was spun up to a 50 g centrifugal acceleration and water was used as a pore fluid.

The finite-difference grid has the discretization depicted in Figure 3a. At the vertical edges of the mesh, the boundary condition of tied nodes was adopted. A pore fluid bulk modulus (for water) equal to $4 \cdot 10^5$ kPa was adopted here, which corresponds to an average saturation ratio $S_r > 99\%$ (e.g., Dashti and Bray, 2013). An additional local damping of 2% was considered in the dynamic analyses to account for the approximately zero

hysteretic damping simulated by the *LiPa* (but also practically any constitutive) model at very small strains. Initially, the geostatic stress field is attained by assuming an earth pressure coefficient at rest K_0 value equal to 0.5 under static equilibrium.

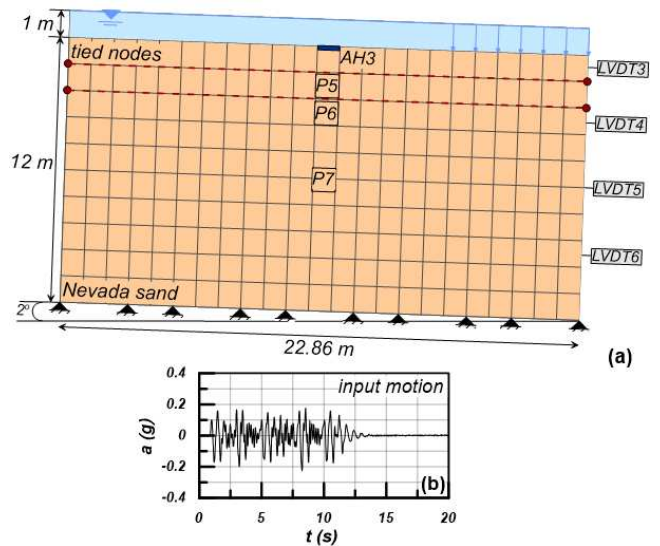


Figure 3. (a) Model layout, discretization, and boundary conditions (b) time-history of horizontal base acceleration

The inclined stress field was induced by applying an extra horizontal gravitational component, which in combination with the vertical one, reproduce the inclined stress field. The resultant vector of gravity is rotated towards the counterclockwise direction by 2° . For Nevada sand with $D_r \approx 40\%$ a permeability coefficient equal to $k \approx 6.5 \cdot 10^{-5}$ m/s is documented at 1g conditions. Since water was used as a pore fluid, to allow for an accurate replication of the experiment performed at a 50 g centrifugal acceleration, the adopted permeability coefficient in the numerical analysis is upscaled by 50 times and then downscaled by 4 times to account for the conflict between the time scales of dynamic pore pressure generation and diffusion during centrifuge experiments (e.g., Popescu and Prevost, 1993). So, if k' is the final permeability coefficient used in the numerical analysis of this test, then $k' = (50/4) k = 8.25 \cdot 10^{-4}$ m/s.

To gain some insight into the effect of post-liquefaction shear strain accumulation on the response, two different modeling scenarios were hereby investigated. This is achieved by changing the value of model constant L_0 . In the first (reference) scenario, the value of $L_0 = 750$ is considered, that is the value calibrated against the element test data for Nevada sand (see Table 1). In the second scenario, a significantly larger value was selected for L_0 ($= 75000$ - Figure 1e), so as the role of the post-liquefaction strain accumulation feature and its intensity to be demonstrated in a BVP involving liquefaction.

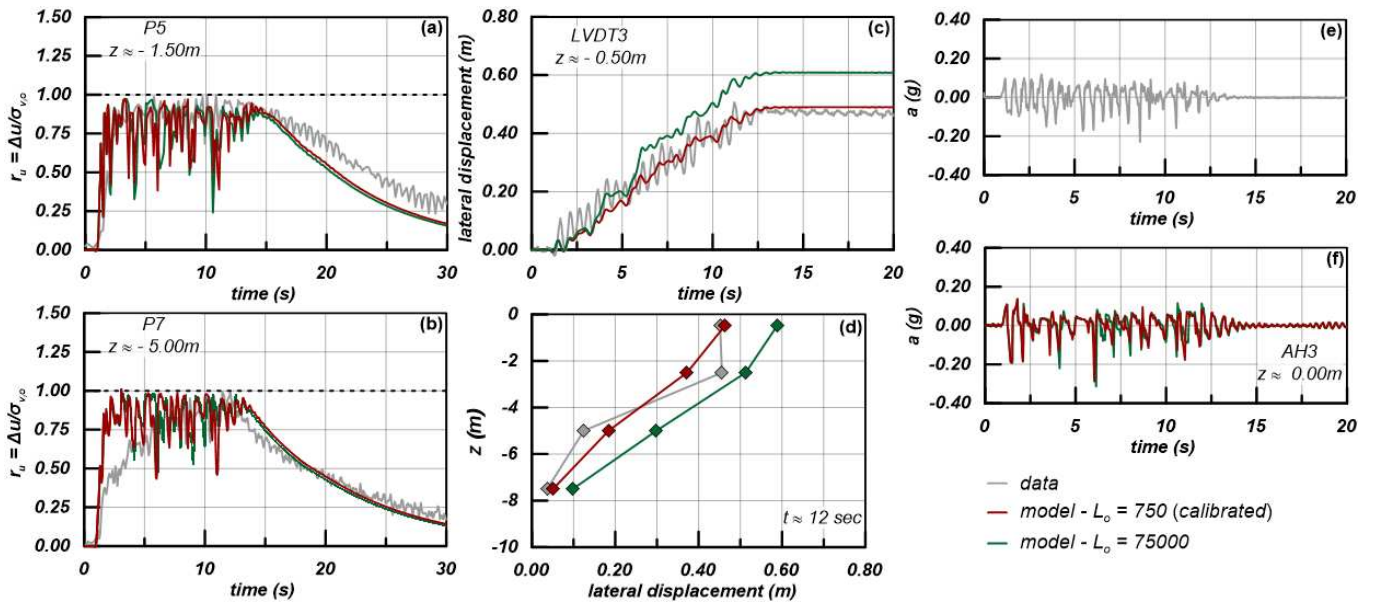


Figure 4. Comparison between data and model simulations in terms of: (a), (b) excess pore pressure time-histories, (c), (d) lateral displacement vs time and depth and (e), (f) horizontal acceleration time-histories

Figure 4 presents comparisons between data and model simulations for VELACS model No. 2. The ruby-red lines refer to the use of the sand-calibrated value of L_o , while the green lines refer to the significantly larger value of L_o . Figures 4a, b present comparisons of time-histories of excess pore pressure ratio r_u for the two indicative locations of P5 and P7 at the axis of the model, which correspond to depths $z \approx -1.5$ m and -5.0 m, with z counting from the ground surface. In general, the simulations are in good agreement with the measurements and the results for the different values of L_o do not show very significant differences, but for slightly more intense pore pressure drops for $L_o = 75000$ that will be related to larger lateral displacements.

Figure 4c compares the measured time-history of lateral displacement with those estimated via the numerical analyses. The results refer to the location of transducer LVDT3. Observe that the accumulation of lateral displacement is practically linear with time, and this is well captured by the model for both calibration scenarios. For the sand-calibrated L_o value, the simulation shows a satisfactory agreement with the data and the surficial displacement is very well estimated. However, for the significantly larger L_o value, there is a clear overestimation of the ground displacements. This means that the more intense post-liquefaction shear strain accumulation (implied by the larger L_o value) translates to larger accumulated (lateral spreading) displacements. Observe that deviations in the two simulations start appearing at $t \approx 2$ s, i.e., when the r_u values obtain a value larger than 0.95 and initial liquefaction is triggered, while, as expected, the pre-liquefaction response is identical. In the sequel, Figure 4d presents a comparison of the lateral displacement data and their numerical estimates from a different perspective. Here, the lateral displacements are compared as snapshots along the whole 10-m thick liquefiable layer at the specific time

instance of $t = 12$ s. For the sand-calibrated L_o value, the comparison with the data is satisfactory. On the contrary, for the significantly larger L_o value, there is an overestimation of the data at all depths of the liquefiable layer.

Finally, Figures 4e, f show a comparison between the recorded and the simulated horizontal acceleration at the position of accelerometer AH3, which is placed near the ground surface ($z \approx -0.25$ m) at the axis of symmetry of the model. Generally, there is a satisfactory agreement, as both the experimentally recorded accelerations and those numerically simulated show a comparable acceleration amplitude near the ground surface. Notably, in both the experiment and the simulations the surface accelerations do not nullify after $r_u \approx 1$ is first reached, and this is due to the dilation spikes that create r_u values relatively lower than 1. Detailed observation reveals also that the analysis with the larger L_o leads to slightly larger accelerations than the analysis with the sand-calibrated L_o value, and this is a result of the comparatively instantly lower r_u values shown in Figures 4a, b.

3.2 Seismic response of a pile group in a mildly inclined three-layered liquefiable soil profile

In this section, the model is validated in a 3D BVP, including a pile group placed in a mildly-inclined liquefiable sand layer, simulating numerically the centrifuge experiment of Pamuk et al. (2007) by using the finite difference code *FLAC3D* (Itasca, 2012). The layout (Figure 5) comprises a 10-m deep three-layered soil system with a 2×2 end-bearing pile group and a pile top-cap. In prototype scale, the stratigraphy includes a bottom layer of 2 m-thick cemented (non-liquefiable) sand, followed by a 6 m-thick uniform liquefiable Nevada sand layer of relative density close to 40%, topped by a 2 m-thick cemented, non-liquefiable sand layer.

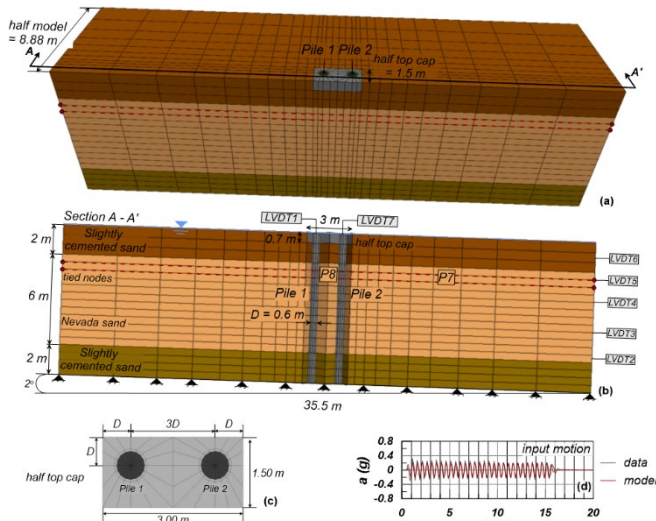


Figure 5. (a), (b), (c) Model layout, discretization, and boundary conditions (d) time-history of horizontal base acceleration

The soil profile has a clockwise inclination of 2° in order to create a mild slope. The actual inclined stress field in this test was simulated in a similar way to that for VELACS Model test No. 2. The pile top-cap had dimensions equal to 3 m (width) x 3 m (length) x 0.7 m (height) in prototype units and was fully embedded in the top cemented sand layer at the center of the box. The piles had a diameter of $D = 0.6$ m in prototype scale and were spaced at a distance of $3D$. Their bending stiffness (EI) was measured 8000 kNm^2 . No information about their installation in the centrifuge experiment was provided, so they were considered as wished in place. The model was built into a 35.5 m (length) x 17.5 m (width) laminar box and was spun up to a 50 g centrifugal acceleration. A sinusoidal input motion was applied horizontally at the base of the laminar box and it consisted of 29 main cycles of frequency equal to 2 Hz and peak acceleration equal to 0.25 g and 2 transitional cycles before and after the main event (Figure 5). Given that the experimental setup is totally symmetrical, it was chosen to simulate the half of the numerical problem.

For the simulation of cemented sand layers and structural elements rational assumptions have been made, since the information in the publication is rather limited. Specifically, both the base and the surficial cemented sand layers were simulated as elastic media, with elastic shear modulus equal to 4350 kPa and a bulk modulus equal to 11300 kPa for the bottom layer and 1450 kPa and 3782 kPa respectively for the surficial layer. For both of these layers, the permeability coefficient k' was considered equal to 10^{-8} m/s , indicating practically impermeable sand layers due to cementation. On the contrary, for the middle liquefiable loose Nevada sand layer a value of k' equal to $8.25 \cdot 10^{-4} \text{ m/s}$ was adopted, following the same rationale of the previous paragraph. Finally, additional local damping of 2% was considered in

the dynamic analyses. The structural elements, including the piles and the top-cap, were simulated also as elastic, while their elastic moduli were chosen to be in accordance with the values of stiffness reported by Pamuk et al. (2007).

Figures 6a, b present a comparison of the time-histories of excess pore pressure ratios r_u between the measured values with pore pressure transducers during the experiment and those given by the numerical analysis at the indicative locations of $P7$ and $P8$, which correspond to the depth of $z = -2.85 \text{ m}$ at the free field and between piles $P1$ and $P2$ respectively. In comparison to the experimental data, the numerical results show good agreement, albeit the analysis estimates less intense dilation spikes than the experiment. Subsequently, Figures 6c, d compare the time-histories of the induced lateral displacement of the surface at the free-field and of the top-cap measured during the experiment and those given by the numerical analysis. The lateral displacement is the result of the lateral spreading of the liquefied loose Nevada sand layer. The comparison is very satisfactory in terms of lateral displacements in both locations throughout the shaking. Figure 6e presents a comparison of the data and the numerical results of lateral displacement of the free-field as snapshot along the whole soil profile depth at the locations of LVDTs 2 - 6 at the specific time moment of $t = 12 \text{ s}$. The comparison is generally satisfactory, with numerical results slightly overestimating the displacements at the lower depths and approaching them at the shallower locations, and thus showing a more curved distribution of lateral displacement with depth. Additionally, Figure 6f compares the recorded and the numerically predicted bending moment that developed along Pile 1 at the specific time moment of $t = 12 \text{ s}$. The numerical results are derived analytically utilizing the induced lateral displacement of the piles. In general, the comparison is quite satisfactory, with numerical results estimating both quantitatively and qualitatively well the developed moments on the piles at all depths. The “S” shaped distribution of the moment with depth and its high values at the interfaces between the loose liquefied Nevada sand layer and the cemented upper and lower sand layers is consistently captured by the analysis.

4 CONCLUSIONS

This paper presents the verification of a new bounding surface plasticity model with reversal surfaces named *LiPa*, when used in boundary value problems (BVPs) related to seismic liquefaction, both in 2D and in 3D space.

After validating the model against element tests on Nevada sand, this paper employs the same set of values of model constants for ascertaining the model's simulative potential at the system level, via comparisons with data from 2 dynamic centrifuge tests performed on the same sand, namely: a) the lateral spreading response of

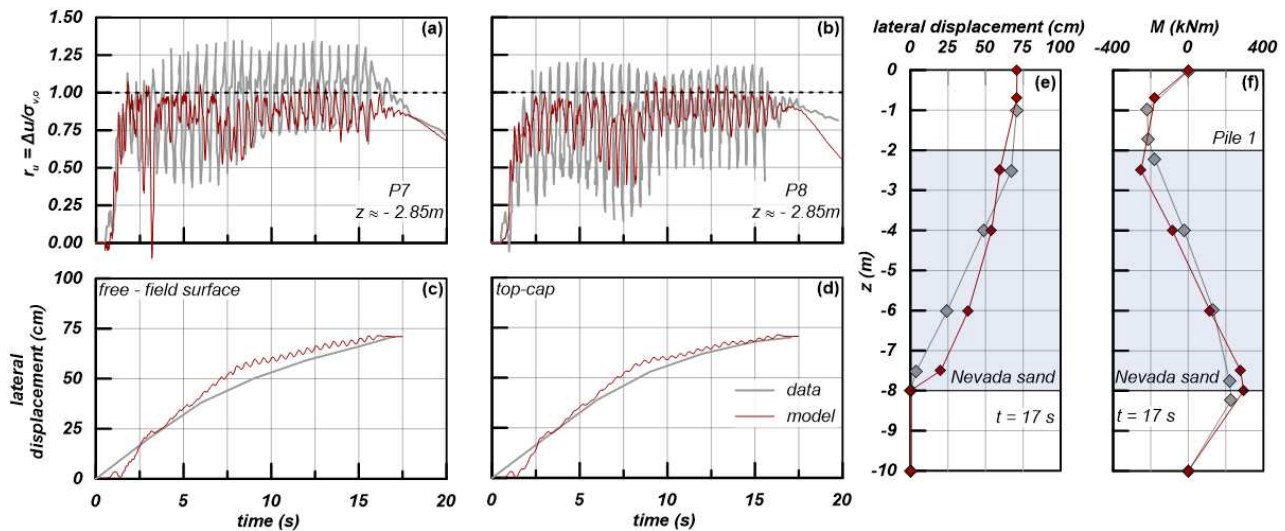


Figure 6. Comparison between data and model simulations in terms of: (a), (b) excess pore pressure timehistories, (c), (d) lateral displacement versus time and (e) versus depth and (f) bending moment on Pile 1.

a gently sloping liquefiable layer and b) the pile group response in a gently sloping liquefiable layer. The model is proven to provide satisfactory accuracy in simulating accelerations, excess pore pressures and lateral displacements of geostuctures in a liquefaction regime, without the need of case-specific re-calibration. Note that this accuracy is achieved with a value of sand permeability coefficient that only depends on the D_r of the sand, i.e., without resorting to approximations of time-dependent (or possibly excess pore pressure ratio - dependent) permeability coefficient due to liquefaction, as often performed in the literature. Additional analyses of these same BVPs show that incorporating a post-liquefaction strain accumulation formulation leads to larger accumulated displacements of geostuctures, without this increase of displacements being overly significant. This means that such formulations, that have started to appear in different forms in sand constitutive models lately, are undoubtedly useful, but their accuracy relies on proper calibration. To be frank, their properly calibrated use does contribute to increased accuracy, but this level of accuracy is not considered crucial for the BVPs involving liquefaction, at least for the hereby adopted scheme.

5 ACKNOWLEDGMENTS

This paper was supported by the Onassis Foundation Scholarship ID: G ZO 013-1/2018-2019, awarded to the first author for her Ph.D. studies.

6 REFERENCES

- Andrianopoulos, K.I., Papadimitriou A.G., Bouckovalas G.D. 2010. Bounding surface plasticity model for the seismic liquefaction analysis of geostuctures. *Soil Dynamics and Earthquake Engineering*, **30**(10), 895-911
- Arulmoli, K., Muraleetharan, K.K., Hossain, M.M., Fruth, L. S. 1992. *VELACS: Verification of liquefaction analysis by centrifuge studies. Laboratory testing program - Soil Data*

- Report*. The Earth Techn Corp, Irvine
- Bouckovalas, G., Whitman, R.V., Marr, W.A. 1984. Permanent displacement of sand with cyclic loading. *J Geotech Eng* **110**, 1606-1623
- Darendeli, M. 2001. *Development of a new family of normalized modulus reduction and material damping curves*. PhD Thesis. The University of Texas at Austin
- Dashti, S., Bray, J.D. 2013. Numerical simulation of building response on liquefiable sand. *J Geotech Geoenviron Eng* **139**, 1235-1249
- Limnaiou, T.G., Papadimitriou, A.G. 2022. Verification of bounding surface plasticity model with reversal surfaces for the analysis of liquefaction problems, *Soil Dynamics and Earthquake Engineering* **163**, 107394
- Limnaiou, T.G., Papadimitriou, A.G. 2023a. Bounding surface plasticity model with reversal surfaces for the monotonic and cyclic shearing of sands, *Acta Geotech* **18**, 235-263.
- Limnaiou, T.G., Papadimitriou, A.G. 2023b. Constitutive model with reversal surfaces for granular soils under monotonic and cyclic loading. *Proceedings, 10th European Conference on NUMGE* (Eds: Zdravković, L., Kontoe, S., Taborada, D.M.G. & Tsiampousi, A.) Imperial College, London
- Kammerer, A.M., Wu, J., Pestana, J.M., Riemer, M., Seed, R.B. 2000. *Cyclic simple shear testing of Nevada sand for PEER Center Project 2051999*. Berkeley, CA.
- Itasca Consulting Group Inc. 2011. *FLAC-Fast Lagrangian Analysis of Continua, version 7.0*. Itasca, Minneapolis.
- Itasca Consulting Group Inc. 2012. *FLAC^{3D}, version 5.0*. Itasca, Minneapolis.
- Pamuk, A., Gallagher, P.M., Zimmie, T.F. 2007. Remediation of piled foundations against lateral spreading by passive site stabilization technique. *Soil Dynamics and Earthquake Engineering* **27**(9), 864-874
- Popescu, R., Prevost, J.H. 1993. Centrifuge validation of a numerical model for dynamic soil liquefaction. *Soil Dynamics and Earthquake Engineering* **12**(2), 73-90.
- Taboada, V., Dobry, R. 1994. Experimental results of model No. 2 at RPI. In: *Proceedings, International Conference on Verification of Numerical Procedures for the Analysis of Soil Liquefaction Problems*, Davis, CA, vol. 1